

Maximizing the Output Power of Advanced Multi-Junction Photovoltaic Devices Through Novel Optimization Algorithm

Sherif Michael

Abstract: In this paper, a novel solar cell structure using 2-Terminal, 3-Cell, Stack (2T3CS) is designed and modeled in Silvaco Atlas to overcome intrinsic limitations of state-of-the-art designs. The primary goal of series connected solar cell design is to maximize the output power for a given solar spectrum. The construction of such tandem cells places the individual cell layers in series, thereby limiting the overall output current to that of the junction layer producing the lowest current. The solution to optimizing a tandem design involves both the design of individual junction layers which produce an optimum output power and the design of a series-stacked configuration of these junction layers which yields the highest possible overall output current and voltage. Genetic search algorithm was introduced to achieve this task. An Indium-Gallium-Phosphide, Gallium-Arsenide and Germanium back-contact solar cells are designed and optimized for current-matching to achieve more than 32 percent power conversion efficiency at AM1.5G (300K) are presented. Two-terminal operation permits a variety of series and/or parallel-connection topologies for module operation. Research is underway to improve efficiency through the use of optimal bandgap materials.

Keywords—solar cell; simulation; modeling; mechanically-stacked

I. INTRODUCTION

Mechanically-stacked (MS) solar cells gained popularity in the early days of cell design before advancements in Metal-Organic Chemical Vapor Deposition (MOCVD) and Epitaxial-Lift-Off (ELO) technology enabled precise fabrication of monolithic multi-junction (MMJ) cells [1]. Although MMJ cells dominate the market for space applications, cost can be prohibitive for terrestrial use. The less-expensive and more straight-forward approach of mechanically joining single-junction (SJ) cells is an attractive alternative, especially for back-contact cells that do not lend themselves to MMJ design.

This work builds upon previous research that introduced patent-pending “Emitter-less, Back-surface, Alternating

Contact (EBAC) solar cell technology [2]–[5]. EBAC technology eliminates the $p-n$ junction associated with the emitter/bulk interface to boost output voltage, employs back-surface contacts to improve photogeneration, and utilizes heterocontacts to selectively accept charge carriers for high-efficiency operation. In this paper, EBAC technology is leveraged in three solar cell designs to produce a novel 2-Terminal, 3-Cell, Mechanical-Stack (2T3CMS) simulated in Silvaco Atlas. Generally, MS designs are leveraged to avoid the requirement to match currents; however, we adopted the MS approach because EBAC technology requires minority and majority carrier transport toward the back surface.

II. SCIENTIFIC INNOVATION AND RELEVANCE

To the best of the authors’ knowledge, a 2T3CMS cell that implements back-contact technology has not been presented before in literature. Additionally, we introduce the first InGaP cell with back-surface contacts to join with the GaAs-EBAC cell introduced in [2]. Finally, an innovative Ge-EBAC cell is designed and simulated to complete the stack. Consequently, the research is relevant as a new method to achieve high-efficiency operation in a three-cell mechanical stack.

III. SOLAR CELL SIMULATION IN SILVACO ATLAS

Silvaco Atlas is a semiconductor device simulator that predicts the electrical characteristics associated with semiconductor structures under bias conditions [6]. The simulator constructs two-dimensional (2D) or 3D physical models and solves differential equations at numerous points throughout the structure to simulate the transport of charge carriers through a device. Physical modeling provides insight into the internal operation of a solar cell and displays data in a visual platform called TonyPlot. GaAs, InGaP and Ge-EBAC cells modeled in Atlas are shown in Figures 1-3.

The author is with the Naval Postgraduate School, Monterey, CA USA

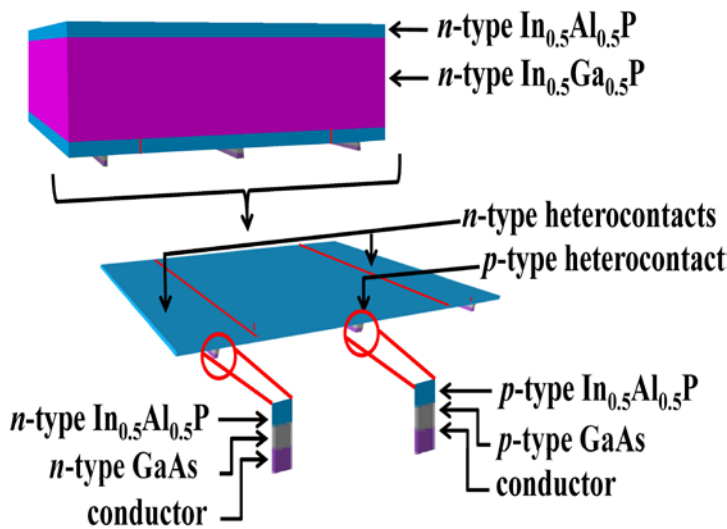


Fig. 1. 3D InGaP-EBAC simulated cell structure.

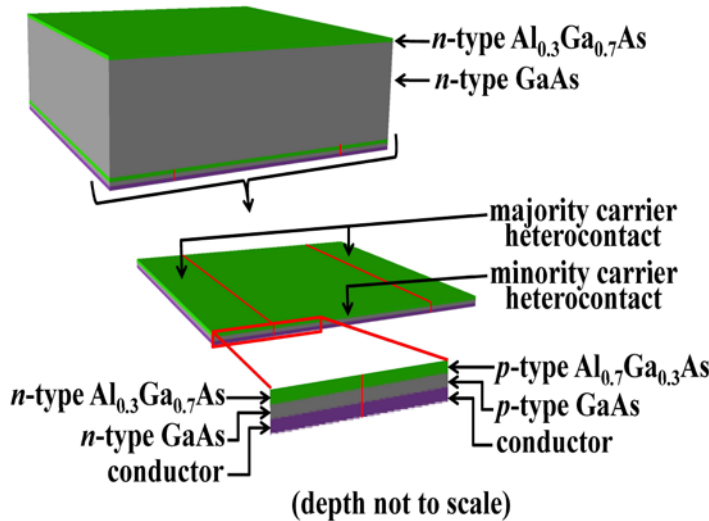


Fig. 2. 3D GaAs-EBAC simulated cell structure.

The back-surface-field is split on either side of the model to produce symmetry, which is important for modeling carrier diffusion in EBAC cells. InGaP-EBAC and GaAs-EBAC cell back-surface contacts are optimally thinned to maximize transparency and minimize resistance.

The 2T3CMS cell is shown in Fig. 4. Silicon epoxy (DC93-500) was simulated using a Dow Corning 7059 glass refractive index available, and semiconductor absorption and extinction coefficients were assigned over each material's spectral range using refractive index data from [7]. Material properties were obtained from [8]-[10]. References [3] and [4] expound experimentally-derived material properties and other important factors important for accurate solar cell simulation. Photogeneration rate in each model was verified

mathematically by calculating photon absorption at various cell depths and comparing results to model output as explained in [1]. A triple-layer coating consisting of MgF2/Al2O3/ZnS was optimized for a 300-1900 nm spectrum and applied to the front surface to minimize external reflection, while single-layer ZnS ARCs were applied at epoxy interfaces to minimize internal reflection. 2T3CMS current-density vs. voltage (J-V) curves are shown in Fig. 5. The appearance of the J-V curves indicates that the Ge-EBAC cell produces more current-density than is required, which suggests that optimization is necessary; however, the lower FF of the Ge-EBAC cell requires additional short-circuit current to produce sufficient current-density at the operating point.

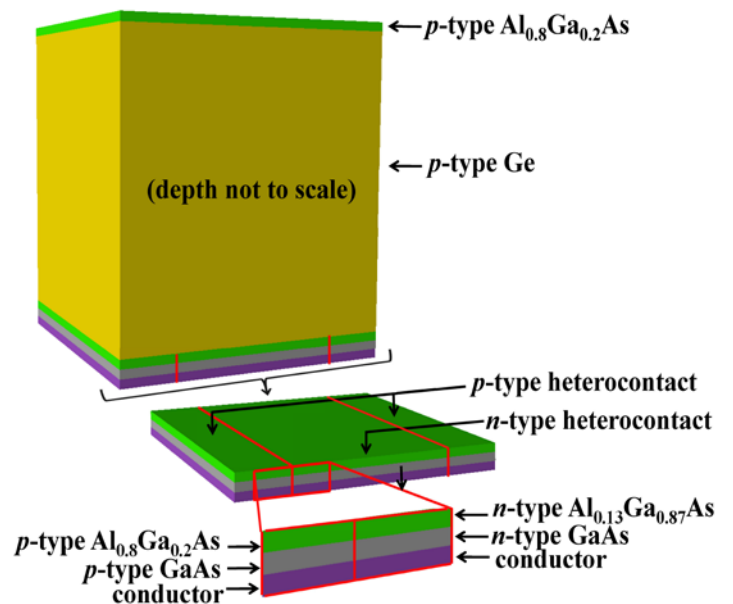


Fig. 3. 3D Ge-EBAC simulated cell structure.

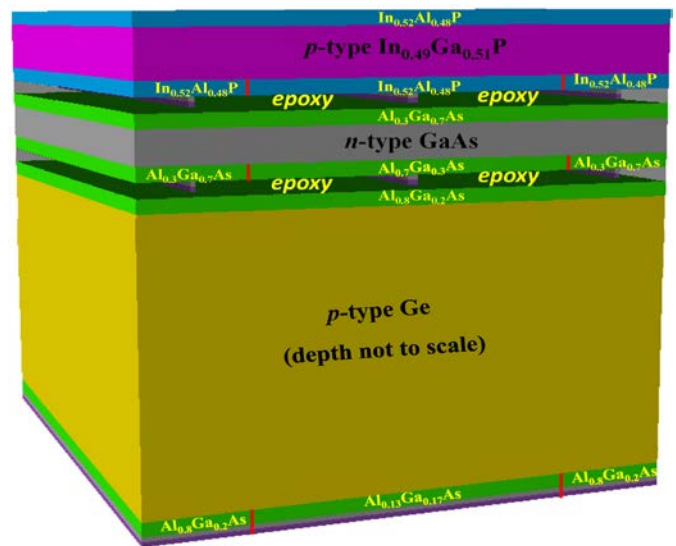


Fig. 4. 2T3CMS simulated structure.

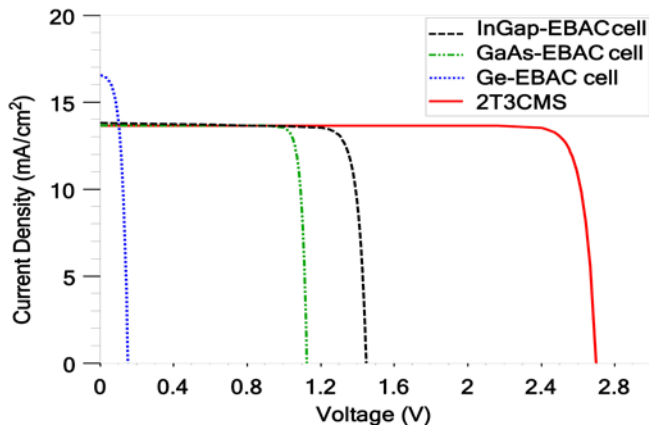


Fig. 5. 2T3CMS simulated output at AM1.5G, 300 K.

IV. THE GENETIC ALGORITHM OPTIMIZATION

A Novel technique using Genetic Search Algorithm was introduced and used to optimize and maximize the output power of the MJ solar cell. The first step in the optimization process is to maximize the output power of each junction layer individually for several layer thicknesses. These optimum configurations will be used to ensure maximum junction layer output power as junction layer thicknesses are changed during the current-matching process. The junction layer optimization process accepts known materials for the window, emitter, base & BSF and determines the ideal thicknesses & dopings for each region. Thus, eight independent variables were used for each overall junction layer thickness. To search all possible solutions rigorously would require an enormous amount of computational time. Instead, a genetic algorithm [8], was used to search the solution space for the junction layer configuration producing the highest output power. To enact a genetic algorithm for junction layer optimization, each of the eight variable junction layer parameters was encoded into a four-bit binary string. The encoded binary strings, referred to as genes, were then assembled into 32-bit binary chromosomes (Fig. 6). Each chromosome fully encoded the eight variable properties of a junction layer. A set of 35 randomly selected binary strings made up the initial generation of chromosomes. The encoded properties in each of these chromosomes were used to construct and simulate a junction layer in ATLAS under AM0 illumination. After the

simulation of an entire generation of chromosomes, child chromosomes (to make up the next generation) were formed from a mix of the genes from the best performing parent chromosomes.

The genetic search algorithm was allowed to progress for a maximum of 20 generations. This scheme allowed a solution space of over 268 million junction layer designs to be searched to arrive near an optimal junction layer configuration for a specific thickness.

V. RESULTS AND DISCUSSION

2T3CMS output parameters at AM1.5G, 300 K after applying the optimization technique are shown in Table I; while output parameters at AM0, 300 K are shown in Table II. The only design characteristics that changed significantly during optimization for the AM0 spectrum was the reduction of InGaP-EBAC cell absorption layer thickness to match currents and enable a dual-terminal connection topology. 2T3CMS External Quantum Efficiency (EQE) is shown in Fig. 7, and spectrum absorption is shown in Fig. 8. Both figures indicate good performance in the 300 to 1900 nm optical wavelength range as expected.

VI. SUMMARY

We presented for the first time an optimized 2T3CMS device with 32.5% and 29.2% power conversion efficiency at AM1.5G and AM0, respectively. We believe that modeling a 2T3CMS device is useful because it demonstrates a path to higher efficiency by enabling the use of EBAC technology in MJ cell design. Efficiency can be further improved by using optimal bandgap materials such as $In_{0.51}Ga_{0.49}P$, $E_G \approx 1.74$ eV; $In_{0.20}Ga_{0.80}As$, $E_G \approx 1.17$ eV; $In_{0.60}Ga_{0.40}As$, $E_G \approx 0.7$ eV. Ideal bandgap semiconductors were not used in this simulation because experimentally derived material properties (i.e. refractive indices, carrier lifetime, etc.) were not available to ensure accurate modeling; however, prototypes fabrication will permit the use of optimal bandgap materials, which is the next step for this research. Genetic Algorithm was introduced to demonstrate Optimization of the MJ device to maximize its overall output power.

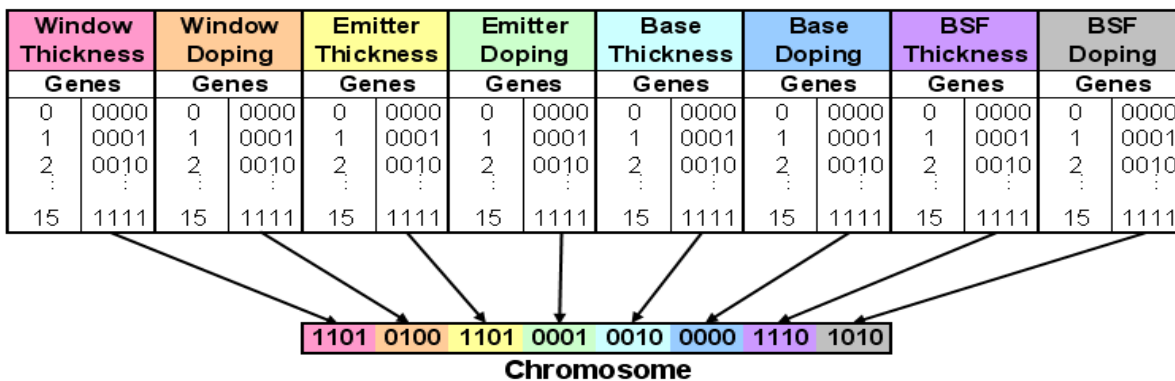


Figure 6. Chromosome construction from a gene sequence.

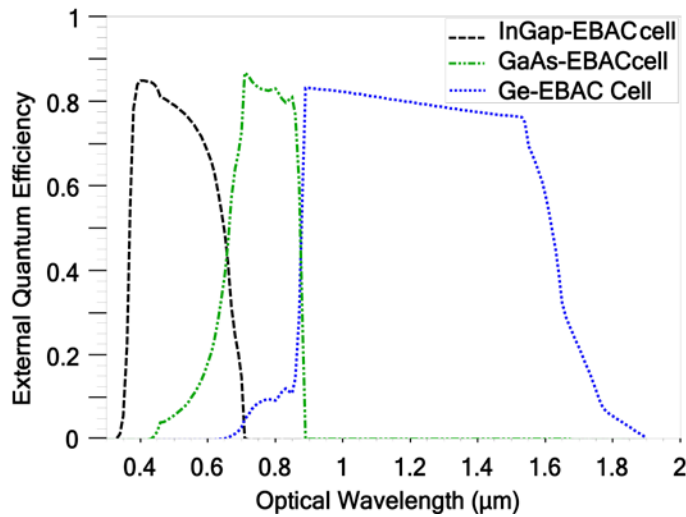


Fig. 7. 2T3CMS external quantum efficiency.

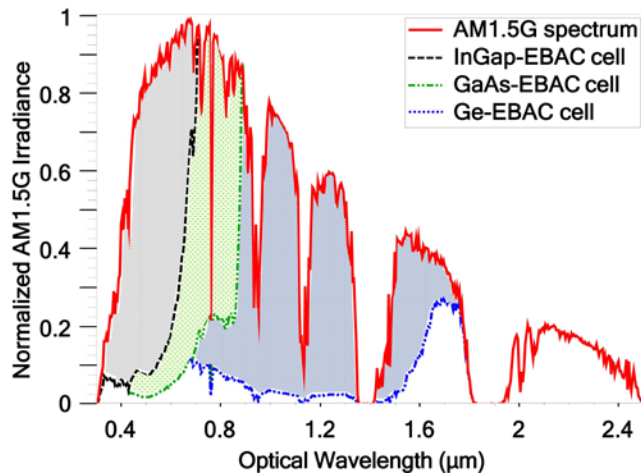


Fig. 8. 2T3CMS AM1.5G spectrum absorption.

TABLE I
2T3CMS OUTPUT PARAMETERS (AM1.5G, 300 K)

Cell	InGaP	GaAs	Ge	2T3CMS
V_{oc} [V]	1.45	1.12	0.16	2.73
V_{MP} [V]	1.31	1.03	0.12	2.46
J_{sc} [mA/cm^2]	13.8	13.7	16.6	13.7
J_{MP} [mA/cm^2]	13.2*	13.3*	13.2*	13.2*
FF [%]	85.8	88.9	58.9	N/A
η [%]	17.2	13.7	1.56	32.5

*current-matched for 2-terminal operation

TABLE II
2T3CMS OUTPUT PARAMETERS (AM0, 300 K)

Cell	InGaP	GaAs	Ge	2T3CMS
V_{oc} [V]	1.45	1.13	0.15	2.73
V_{MP} [V]	1.31	1.03	0.11	2.45
J_{sc} [mA/cm^2]	16.6	16.6	23.0	16.6
J_{MP} [mA/cm^2]	16.1*	16.2*	18.3*	16.1*
FF [%]	87.0	89.0	58.0	N/A
η [%]	15.6	12.4	1.49	29.2

*current-matched for 2-terminal operation

REFERENCES

- [1] L. Zhao, "High efficiency mechanically stacked multi-junction solar cells for concentrator photovoltaics," Ph.D. dissertation, Technical KU Leuven, Leuven, Belgium, 2011.
- [2] J. O'Connor and S. Michael, "A novel, single-junction solar cell design to achieve power conversion efficiency above 30 percent," J. of Materials Science and Applications, vol. 7, no. 12, pp. 823–835, 2016.
- [3] J. O'Connor and S. Michael, "Optimizing a single-absorption-layer thin-film solar cell model to achieve 31% efficiency," J. of Materials Science and Chemical Engineering, vol. 5, no. 1, pp. 54–60, 2017.
- [4] S. Michael and J. O'Connor, "AlGaAs/GaAs solar cell with back-surface alternating contacts," U.S. Patent App. 15-207-128, 4 May 2016.
- [5] J. O'Connor and S. Michael, "Emitter-less, back-surface, alternating-contact solar cell," U.S. Patent App. 15-282-460, 30 Sep 2016.
- [6] Silvaco. (2016, Aug. 30). Atlas user's manual.
- [7] Sopra SA. (n.d.). Optical Data from Sopra SA. [Online]. Available: <http://sspectra.com/sopra.html>
- [8] Ioffe Physico-Technical Institute. (n.d.). New semiconductor materials. Characteristics and properties. [Online]. Available: <http://www.ioffe.ru/SVA/NSM/>
- [9] M. Levinshtein, S. Rumyantsev and M. Shur, Si, Ge, C: Diamond, GaAs, GaP, GaSb, InAs, InP, InSb, Handbook Series on Semiconductor Parameters, vol. 1. Singapore: World Scientific, 1996, p. 218.
- [10] S. Sze and K. Ng, Physics of Semiconductor Devices. 3rd Ed., New York, NY: John Wiley & Sons, 2000.